Metal and Ceramic Thin Film Growth by Reaction of Alkali Metals with Metal Halides: A New Route for Low-Temperature Chemical Vapor Deposition

Jay H. Hendricks,† Maria I. Aquino, James E. Maslar, and Michael R. Zachariah*

National Institute of Standards and Technology, Process Measurements Division, Gaithersburg, Maryland 20899

Received March 17, 1998. Revised Manuscript Received June 15, 1998

A new low-temperature chemical vapor deposition (CVD) method for the growth of metal and ceramic thin films has been demonstrated. This method involves the use of a low-pressure coflow diffusion reactor to react alkali metal vapor with metal halide vapor. The reaction chemistry is described by the following general equation: $mn\mathrm{Na} + n\mathrm{MX}_m \xrightarrow{\mathrm{Ar}} \mathrm{M}_n + nm\mathrm{NaX}$. Here, Na is an alkali metal (e.g. Na, K, Cs, or Rb), M is a metal (e.g. Ti, Ta, Pt, W, ...) or nonmetal (e.g. B, C, Si, ...), X is a halogen (e.g. F, Cl, Br, or I), Ar is an inert gas (e.g. Ar or He), and m and n are integers. In this reaction, the alkali metal strips halogen from the metal halide. The metal is then free to grow into a thin film on a substrate placed in the reaction zone. Metal nitride or metal oxide ceramic films are easily formed by the introduction of nitrogen or oxygen gases into the reactor. Previously, this technique has been successfully employed for the production of nanoparticles and as an industrial synthesis route for the reduction of bulk metals from their metal halides. Now, for the first time, this reaction chemistry has been demonstrated to be a viable technique for thin film growth as well. Using the precursors of sodium metal vapor, titanium tetrachloride (the limiting reagent), and either Ar or N_2 gas, salt-free titanium (Ti), titanium nitride (TiN), and titanium silicide (Ti_xSi_y) thin films have been grown on copper and silicon substrates. Guided by theoretical modeling calculations, reactant concentrations were adjusted to prevent gas-phase particle nucleation and growth. Using this technique, we have produced salt-free titanium and titanium nitride thin films on copper substrates heated to 610 °C. This temperature is considerably lower than the 900−1200 °C required for the conventional thermal CVD of titanium. A composite salt/Ti film was grown on a silicon wafer at 260 °C, while at 610 °C, a salt-free titanium silicide thin film was produced. The quality and composition of the thin films were analyzed by scanning electron microscopy (SEM), energy dispersive spectrometry (EDS), X-ray diffraction (XRD), Raman spectroscopy, and transmission electron microscopy (TEM).

Introduction

The worldwide market for chemical vapor deposition (CVD) equipment and services is projected to grow from $3.5 billion (per year) in 1995 to $5.4 billion by the year 2000.[1] The two major industrial sectors are (a) microelectronics, which currently accounts for approximately 80% of the market, and (b) surface coatings applications (surface hardness enhancement, corrosion inhibition, and medical), which accounts for the remaining 20% of the market. The microelectronics industry is concerned with stringent purity requirements,[2] while the surface coatings industry is primarily concerned with surface hardening (for machine tooling) and surface coating (for corrosion inhibition and medical applications).[3,4] While the microelectronics industry can incur a significant expense to produce a high-purity film with exacting electrical performance, many surface enhancement applications cannot tolerate the high production costs typical of the present-day CVD techniques. Additional challenges that both industries face are the expense of disposing of CVD byproducts and the high surface temperature requirement for many conventional CVD processes (900−1200 °C for thermal CVD of titanium).[5] This latter point is of significance because many substrate materials may not be capable of accepting high deposition temperatures. For example, steel (containing

† NIST NRC Postdoctoral Fellow.
* Corresponding author. E-mail: MRZ@tiber.nist.gov.

(1) Ortelli, G., Ed. *Ind. Ceramics* **1997**, *17*, 45.
(2) Yokohama, N.; Hinode, K.; Homma, Y. *J. Electrochem. Soc.* **1989**, *136*, 882. Yokohama, N.; Hinode, K.; Homma, Y. *J. Electrochem. Soc.* **1991**, *138*, 190.
(3) Rebenne, H. E.; Bhat, D. G. *Surf. Coat. Technol.* **1994**, *63*, 1. Yee, K. K. *Int. Met. Rev.* **1978**, *23*, 19.
(4) Jayaweera, P.; Lowe, D. M.; Sanjurjo, A.; Lau, K. H.; Jiang, L. *Surf. Coat. Technol.* **1996**, *86−87*, 525. Lunarska, E.; Michalski, J. *J. Mater. Sci.* **1995**, *30*, 4125.
(5) Hocking, M. G.; Vasantasree, V.; Sidky, P. S. *Metallic and Ceramic Coatings: Production, High-Temperature Properties and Applications;* John Wiley and Sons: New York, 1989; p 103.

S0897-4756(98)00161-6 This article not subject to U.S. Copyright. Published 1998 by the American Chemical Society
Published on Web 07/30/1998

less than 0.25% C) undergoes a phase transition at 723 °C.[6] In this paper, we present a CVD process which has the benefits of (a) operating at lower temperature than conventional CVD, (b) being of low cost, and (c) being environmentally benign.

The general chemistry used to grow the thin films is outlined in eq 1 below:

$$mn\mathrm{Na} + n\mathrm{MX}_m \xrightarrow{\mathrm{Ar}} \mathrm{M}_n + nm\mathrm{NaX} \qquad (1)$$

Here, Na is sodium (or other alkali metal) and MX_m is a metal-halide (M is a metal or other element such as Si or C, X is a halogen atom, and m and n are integers). This chemistry is spontaneous and was first noted in 1887 by Nilson and Petterson[7] for the reduction of $TiCl_4$ to produce bulk titanium metal. Recently, this chemistry has been demonstrated to be useful for a variety of applications including the synthesis of Ti nanoparticles[8] and TiB_2 nanoparticles,[9] for the formation of an iron/salt magnetic nanocomposites,[10] for the synthesis of high purity Si (near photovoltaic grade),[11] and for the remediation of chlorinated fluorocarbons (CFCs).[12]

Alkali metals, sodium and potassium, have not been used in industrial CVD applications primarily because their high reductive power tends to cause premature and detrimental gas-phase particle precipitation. Furthermore, the incorporation of salt into the deposited metal film is problematic in that high temperatures are required to volatilize and remove the deposited salt.[13] With this in mind, we have set out to demonstrate that a gas-phase alkali metal/metal halide reaction can be run under conditions which are undersaturated in salt and in which a low temperature (610 °C) salt-free metal or ceramic thin film can be grown. The high reductive power of sodium (or other alkali metal) now becomes a benefit in that the thermodynamics so strongly favors the production of salt that there is no inherent need to heat the substrate in order to drive the reaction chemistry (as is typically done in many CVD processes). To avoid problematic gas-phase particle formation and salt deposition, dilute reactant concentrations and moderate substrate temperatures were utilized, allowing us to produce salt-free film.

In this paper, we report for the first time the use of gas-phase alkali metal/metal halide chemistry for the production of thin metal and ceramic films. We feel that

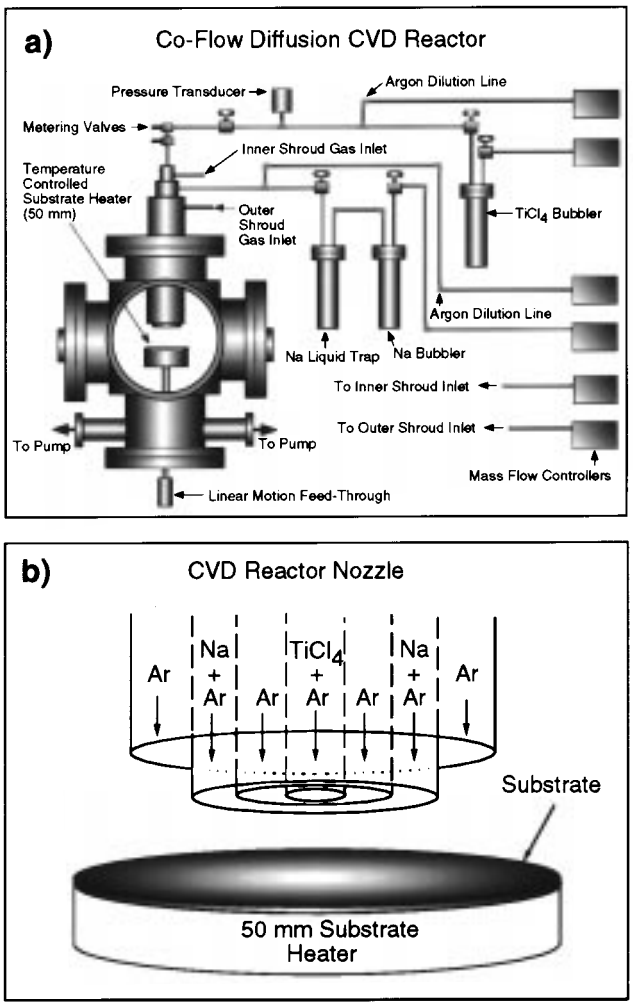

Figure 1. (a) Schematic of the low-pressure coflow diffusion CVD reactor used to react alkali metal vapor with metal halide vapor to deposit metal and ceramic films. Typical reactor conditions are listed in Table 1. (b) Schematic of the reactor nozzle consisting four concentric stainless steel tubes having dimensions of (i.d/o.d) 5.38 mm/6.35 mm, 14.22 mm/15.88 mm, 24.13 mm/25.15 mm, and 36.07 mm/37.95 mm. The injection of reactants is as shown above.

successful implementation of this technique will lead to thin film growth of a wide variety of useful materials, at low cost, and allow operation at lower than conventional CVD temperatures. Finally, this technique has the additional advantage that the byproducts of the thin film growth process are solid phase salts which are easy to capture and are environmentally benign.

Film Growth Apparatus

The following prototype reactions were investigated to demonstrate that the spontaneous gas-phase alkali metal/metal halide chemistry could be used for the production of metal and ceramic thin films:

$$4\mathrm{Na(g)} + \mathrm{TiCl_4(g)} \xrightarrow{\mathrm{Ar}} 4\mathrm{NaCl(g)} + \mathrm{Ti(s)} \qquad (2)$$

$$4\mathrm{Na(g)} + \mathrm{TiCl_4(g)} \xrightarrow{\mathrm{Ar/N_2}} 4\mathrm{NaCl(g)} + \mathrm{TiN(s)} \qquad (3)$$

In this global reaction, Na strips Cl atoms from $TiCl_4$ (typically run as the limiting reagent), leaving Ti atoms

(6) Camp, J. M.; Francis, C. B. *The Making Shaping and Treating of Steel;* United States Steel Company: Pittsburgh, PA, 1951; p 1203. Minkoff, I. *The Physical Metallurgy of Cast Iron;* New York: New York, 1983; p 29.

(7) Nilson, L. F.; Petterson, O. Z. *Physik. Chem.* **1887**, *27* 1. Sittig, M. *Sodium: Its Manufacture, Properties and Uses;* Reinhold Publishing Corp.: New York, 1956; p 213.

(8) DuFaux, D. P.; Axelbaum, R. L. *Combustion Flame* **1995**, *100*, 350.

(9) Axelbaum, R. L.; DuFaux, D. P.; Frey, C. A.; Kelton, K. F.; Lawton, S. A.; Rosen, L. J.; Sastry, S. M. L. *J. Mater. Res.* **1996**, *11*, 948. Steffens, K. L.; Zachariah, M. R.; DuFaux, D. P.; Axelbaum, R. L. *Chem. Mater.* **1996**, *8*, 1871.

(10) Gorshkov, N.; Aquino, M. I.; Shull, R. D.; Shapiro, A.; Zachariah, M. R. *Nanostructured Mater.* **1998**, submitted.

(11) Calcote, H. F.; Felder, W., *Twenty-Forth Symposium (International) on Combustion;* The Combustion Institute: Pittsburgh, PA, 1992; Vol. II.

(12) DuFaux, D. P.; Zachariah, M. R. *Environ. Sci. Technol.* **1997**, *31*, 223.

(13) Pierson, H. O. *Handbook of Chemical Vapor Deposition (CVD): Principles, Technology, and Applications;* Noyes Publications: Park Ridge, NJ, 1992; p 55.

Table 1. Coflow Diffusion CVD Reactor Conditions

sample code	coating film	substrate material	reactant gases	pres., Pa	N_2(g), slpm[a]	Ar(g), slpm[a]	$TiCl_4$(g), sccm[b]	Na(g), sccm[b]	ratio Na/Cl	time, h[c]	T, °C[d]	vel, cm/s[e]
R23	Ti+NaCl	Si⟨100⟩	Na, Ar, $TiCl_4$	800	0.0	3.6	2.9×10^{-3}	1.2×10^{-2}	1.1	6.5	435	1900
R11	Ti+NaCl	Si⟨100⟩	Na, Ar, $TiCl_4$	800	0.0	3.6	2.9×10^{-3}	5.1×10^{-2}	4.4	4.0	260	1900
R23W	Ti	Si⟨100⟩	Na, Ar, $TiCl_4$	800	0.0	3.6	2.9×10^{-3}	1.2×10^{-2}	1.1	6.5	435	1900
R22	Ti_xSi_y	Si⟨100⟩	Na, Ar, $TiCl_4$	800	0.0	3.6	2.9×10^{-3}	1.6×10^{-2}	1.4	5.2	600	1900
R15	none	Si⟨100⟩	Ar, $TiCl_4$	800	0.0	3.6	2.9×10^{-3}	none	0.0	5.5	600	1900
R26	Ti	OFHC Cu	Na, Ar, $TiCl_4$	800	0.0	3.6	1.0×10^{-3}	1.6×10^{-2}	4.0	6.5	610	1900
R29	TiN	OFHC Cu	Na, Ar, N_2, $TiCl_4$	800	0.1	3.5	3.3×10^{-3}	5.3×10^{-2}	4.0	5.5	610	1900

[a] Standard liters per minute. [b] Standard cubic centimeters per minute. [c] Deposition time. [d] Substrate temperature. [e] Reactant exit velocity.

free to nucleate and grow into a thin film at the substrate surface. Theoretical modeling calculations[14] and in situ optical investigations of the reaction chemistry[15] were used to guide both the design and the operational conditions of the reactor so that gas-phase nanoparticle formation could be suppressed.

The apparatus (shown schematically in Figure 1) consists of a stainless steel chamber, a nozzle for the introduction of reactants, a temperature-programmable substrate heater, a pressure-regulated pumping system, and a bank of six mass flow controllers (see Figure 1a). High purity argon (99.998) was further purified by passing the gas through a home-built oxygen scrubber consisting of a stainless steel tube packed with copper turnings maintained at 625 °C. The Ar was then passed through a dual stage water/oxygen gas scrubber before entering a gas manifold that supplies six mass flow controllers. The mass flow controllers were used to meter the flow of Ar, $TiCl_4$, and Na entering the reaction chamber through a reaction nozzle. The reaction nozzle consists of a series of concentric tubes (see Figure 1b). The reaction nozzle's center annulus delivered a metered Ar/$TiCl_4$ mixture that was prepared by bubbling 0.25−0.11 standard cubic centimeters per minute (sccm) of argon gas through liquid $TiCl_4$ at room temperature (21 °C) and then additionally diluting this stream with 85 sccm of argon. A pressure transducer was used in conjunction with two stainless steel metering valves to maintain a constant pressure of 1.04×10^5 Pa (760 Torr) in the $TiCl_4$ bubbler, irrespective of the reaction chamber pressure. Sodium vapor was generated by flowing 2−10 sccm of argon through a liquid sodium bubbler held at a constant temperature between 300 and 500 °C. The sodium saturated argon flow was further diluted with 915 sccm of argon before being injected into the reaction chamber via the third reaction nozzle annulus. An argon gas flow of 615 sccm, injected into the reaction chamber via the second reaction nozzle annulus between the $TiCl_4$ and Na flow streams, prevented the reaction chemistry from occurring at, or inside, the reaction nozzle. A final outer shroud of 2000 sccm of argon injected into the reaction chamber via the fourth annulus of the reaction nozzle confined the reaction zone, streamlined the reactive flow, and prevented outside contaminants from entering the reaction zone. The latter point is important, as the purity of the reaction zone is only limited by the purity of the input gases, and is not dependent on an ultrahigh vacuum (UHV) pumping system. The chamber was held at a constant pressure of 800 Pa (6.00 Torr) with an automated exhaust throttle control valve. At 800 Pa, the average exit velocity of all reactants and shroud gases was 1900 cm/s with a Reynolds number of ∼144 and reactant residence time of 2.8 ms. The molar concentration of sodium vapor at the jet exit was held constant at values between 1.3×10^{-5} and 3.0×10^{-5}, while the molar concentration of $TiCl_4$ was held constant at values between 1.6×10^{-5} and 3.2×10^{-5} (the Na/Cl ratio was fixed at values between 1.1 and 4.4 for all experimental runs). Under these conditions, a typical film deposition rate of ∼0.1 μm/h is expected (which is in agreement with preliminary wavelength dispersive spectrometer (WDS) results showing a film thicknesses of ∼0.5 μm for films deposited over a 6 h time period). A 50 mm diameter temperature-controlled substrate heater was held on a linear-motion feed-through 38−50 mm beneath the reaction nozzle (the reactor geometry could be scaled-up to handle larger substrate sizes as needed). The substrate temperature and position were thus precisely maintained and easily varied. Quartz windows on the front and side of the reactor allowed the film growth to be monitored visually.

(14) Zacahariah, M. R., results to be published.

Film Growth Results and Discussion

A series of experiments were conducted to determine if the reaction chemistry shown in eqs 2 and 3 could be used to grow thin titanium and titanium nitride films without the deposition of salt (NaCl). A variety of substrate temperatures, reactant concentrations, and substrate materials were used in the coflow diffusion CVD reactor, and these conditions are summarized in Table 1.

A. Ti Deposition on Si⟨100⟩. Silicon wafers, Si⟨100⟩, were initially chosen as an easily obtainable, relatively inexpensive, and high-quality deposition substrate. The native SiO_2 layer was removed by following a "modified RCA cleaning procedure".[16] In the final step of this cleaning procedure, the wafer was dipped in a dilute HF solution (50:1 HF:H_2O) and then immediately dried, leaving the dangling silicon bonds of the wafer surface hydrogen-terminated.[17] Immediately after etching, the wafer was loaded into the coflow CVD reactor. A small amount of suspended silver conductive paste was applied to one side of the wafer to ensure good thermal conductivity between the substrate heater and the

(15) Steffens, K. L.; Zachariah, M. R., DuFaux, D. P., Axelbaum, R. L. *Chem. Mater.* **1996**, *8*, 1871. Scurlock, C. T.; Axelbaum, R. L.; Zachariah, M. R. results to be published.

(16) Kern, W. *RCA Rev.* **1970**, *31*, 187. Taubenblatt, M. A., Ph.D. Thesis, Stanford University, p 38, 1985.

(17) Atluri, V.; Herbots, N.; Dagel, D.; Bhagvat, S.; Whaley, S. *Nuclear Instrum. Methods Phys. Res. B.* **1996**, *118*, 144.

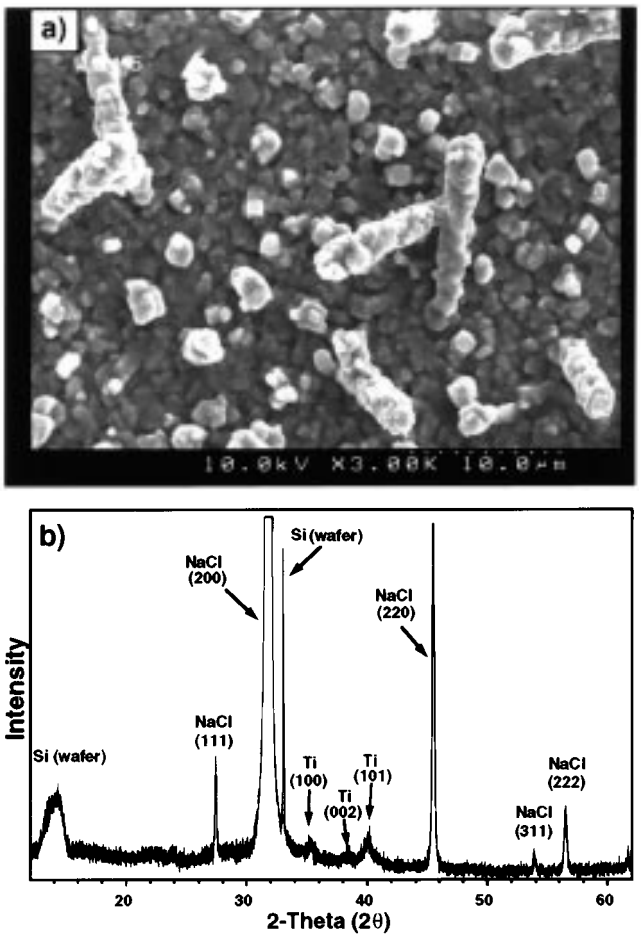

Figure 2. (a) Scanning electron micrograph (SEM) of sample R23 (see Table 1 for reactor conditions). A 435 °C Si⟨100⟩ substrate was used for the deposition surface. This image shows NaCl + Ti deposits. The tall columnar structures are likely to be salt, and their size and shape indicates a surface growth mechanism. (b) X-ray diffraction (XRD) spectrum of sample R23 showing the presence of both NaCl and Ti metal.

wafer. The hydrogen-terminated layer was desorbed by briefly heating the wafer to 600 °C under vacuum.[18] Figure 2a shows the scanning electron microscope (SEM) image of the film obtained from run R23. The sample was prepared with a substrate temperature of 435 °C at a reactor pressure of 800 Pa for 6.5 h. The image shows that the film is composed of aggregates ranging in size from 1 to 10 μm. X-ray diffraction (XRD) shown in Figure 2b shows the presence of crystalline sodium chloride and crystalline Ti. The XRD spectrum also showed structure from the underlying silicon substrate (determined by XRD analysis of a cleaned silicon ⟨100⟩ wafer blank). The presence of salt confirms that reaction 2 was indeed proceeding and that the $TiCl_4$ was reacting with the sodium to release Ti metal and sodium chloride.

Given that the aim of these experiments was to examine the reaction parameters which affected film morphology and salt deposition, lower substrate temperatures were further explored. Sample R11 was run with a Si⟨100⟩ substrate temperature of 260 °C. As expected, this resulted in enhanced salt deposition.

(18) Gates, S. M.; Kunz, R. R.; Greenlief, C. M. *Surf. Sci.* **1989**, *207*, 364.

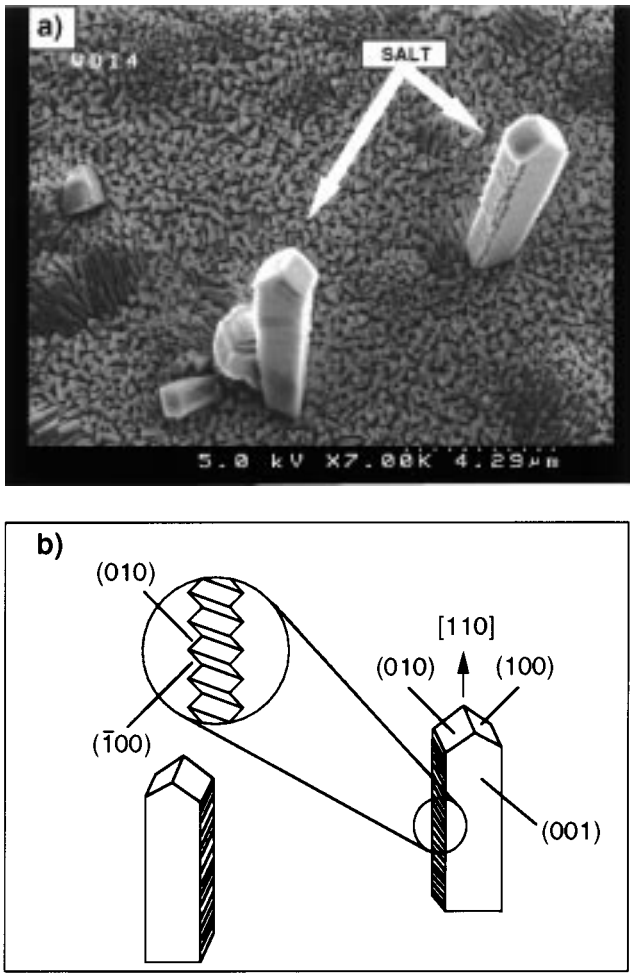

Figure 3. (a) SEM image of sample R11 (see Table 1 for reactor conditions). A 260 °C Si⟨100⟩ substrate was used for the deposition surface. The tall towers are pillars of NaCl. The lower substrate temperature has increased the amount of salt deposited on the substrate surface. XRD analysis of this film confirmed the overwhelming presence of salt (NaCl). (b) Schematic representation of salt "towers". The edge of the salt tower shows that faceted crystal growth has occurred along the (100) planes. The tower shape appears to be due to rapid growth along the [110] direction orthogonal to the substrate surface.

Shown in Figure 3a is a SEM image of the resulting film, revealing remarkable salt "towers". XRD and electron dispersive spectroscopy (EDS) analysis of this film confirmed the overwhelming presence of NaCl (salt). While not the current focus of the work, these "self-assembled" salt structures pose many interesting questions as to the nature of the growth mechanism. The edge of the salt tower (Figure 3a,b) clearly shows that faceted crystal growth has occurred. The tower shape appears to be due to rapid growth along the [110] direction orthogonal to the substrate surface.

Since salt is highly soluble in water, an experiment was conducted to determine if the salt that codeposited with the titanium in sample R23 could be removed by washing the substrate in water. The film was soaked overnight in preboiled room temperature distilled and deionized water. X-ray analysis of the postwashed film revealed that the salt had been removed, as can be seen by the absence of NaCl peaks in the X-ray diffraction pattern (see Figure 4a). The insert in Figure 4a shows clearly the presence of Ti, and from the full-width-at-

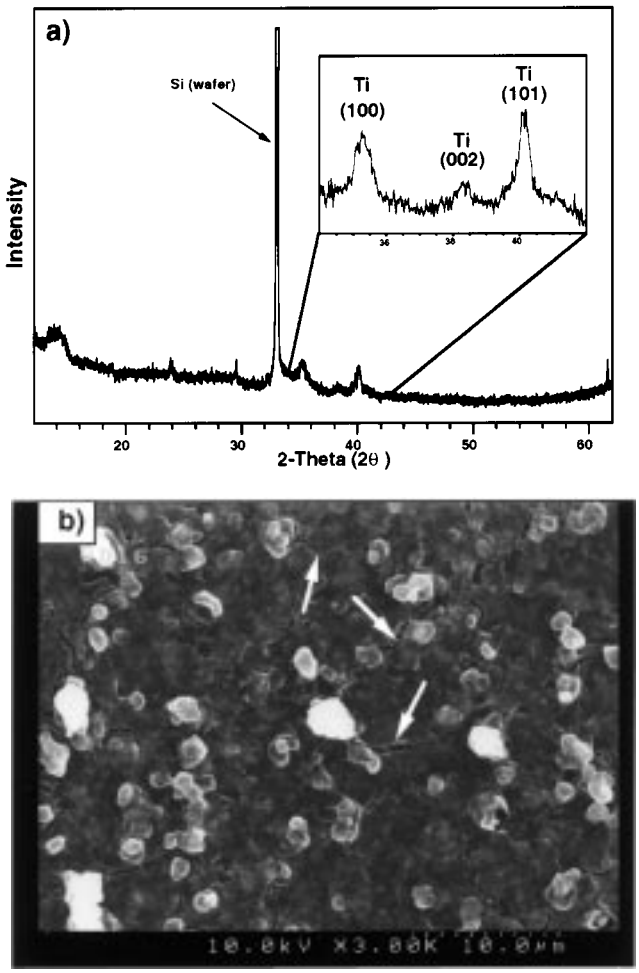

Figure 4. (a) XRD spectrum of sample R23W (the film remaining on the Si⟨100⟩ substrate after rinsing sample R23 with water). X-ray analysis shows clearly the presence of titanium (see inset). All previously detectable salt peaks (see Figure 2b) are no longer present. (b) SEM image of sample R23W showing that the columnar structures shown in Figure 2a are now absent (further evidence that the columnar structures were primarily composed of NaCl). Note that cracking of the film is evident and is probably caused by film stress due to dissolving of salt from the film matrix.

half-maximum (fwhm) of the peak centered at $2\theta = 40.17°$, a crystallite size of 20 nm is inferred from the Scherrer equation.[19] While washing the film removes excess salt, it is unlikely to produce a high-quality titanium film. Cracks are visible in the SEM image of the postwashed film (see Figure 4b), indicating that removal of the salt has stressed the film surface. A transmission electron microscope (TEM) image of the film showed that the particles were between 1 and 10 nm, which compared reasonably well with the 20 nm crystallite size determined by XRD. Energy dispersive spectrometry (EDS) revealed the presence of O, Ti, Fe, and Cu. The copper signal was from the TEM grid, and the oxygen is probably due to titanium oxides that formed when the sample was handled in air and washed with water. The presence of Fe is not as clear and is likely to be an impurity in the $TiCl_4$ liquid feed-

(19) Warren, B. E. *X-ray Diffraction*; Dover Publications: New York, 1990; p 253. Note: The Scherrer equation does not yield highly accurate determinations of particle size and tends to overestimate the particle size at low angles of 2θ.

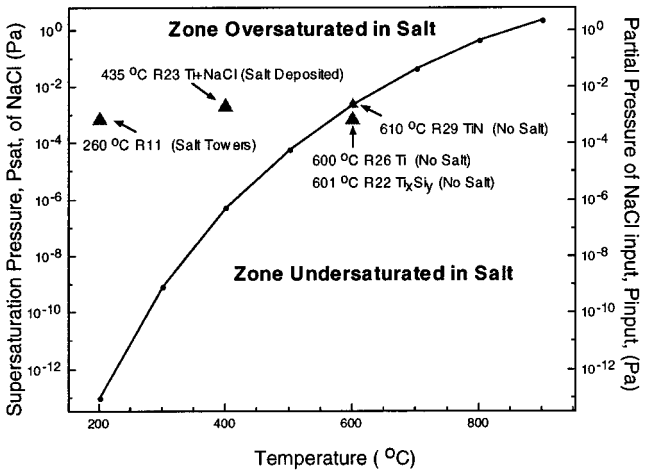

Figure 5. Plot of the supersaturation pressure of NaCl in the reaction zone (P_{sat}) (left-hand axis) versus temperature and the plot the partial pressure of salt input (P_{input}) (right-hand axis) versus temperature. The area above the solid curve should be oversaturated in salt (salt will deposit on the film), while area under the curve will be undersaturated in salt (salt will not deposit on the film). The solid curve was determined from thermodynamics calculations[14] and the triangles are individual experimentally determined points from the reaction conditions (substrate temperature and $TiCl_4$ input into the reaction zone).

stock. The selected area electron diffraction (SAED) pattern showed that a polycrystalline structure was present.

Previously, Ti nanoparticles encased in a salt shell were produced by reacting $TiCl_4$ and Na in a coflow flame reactor.[8] It was found that the salt coating arrested further growth of the Ti nanoparticles. While this effect is desirable for the production of nanoparticles (it can be used to control size, shape, and degree of agglomeration), it is not desirable for thin film growth.[13] Therefore, finding reaction conditions which minimize the amount of deposited salt were sought.

B. Ti Deposited at Lower Supersaturation of Salt on Si⟨100⟩ Substrates. Having demonstrated that the vapor phase chemistry could be driven at low temperatures, the next aspect of the work was to show that a film could be deposited under reactor conditions which were undersaturated in the salt concentration. Having the substrate at higher temperatures should increase the vapor pressure of the salt and lead to a salt-free titanium film. Thermodynamics calculations[14] indicated that, under the reactant concentrations we were employing, a substrate temperature of 600 °C would produce salt-free film. Shown in Figure 5 is a plot of the partial pressure of salt vs temperature determined from the thermodynamics calculations. Reaction conditions falling on points above the solid line are oversaturated in salt (salt will deposit on the substrate), while those below it will be undersaturated in salt (salt will not deposit on the substrate). The concentration of salt input into the reaction zone for individual runs was determined by assuming 100% reaction of $TiCl_4$ ($TiCl_4$ was the limiting reagent). Figure 5 shows that samples R11 and R23 were run with conditions which were oversaturated in salt, leading to salt contaminated films. Samples R22 and R26 were run with higher substrate temperatures and should therefore be salt-free.

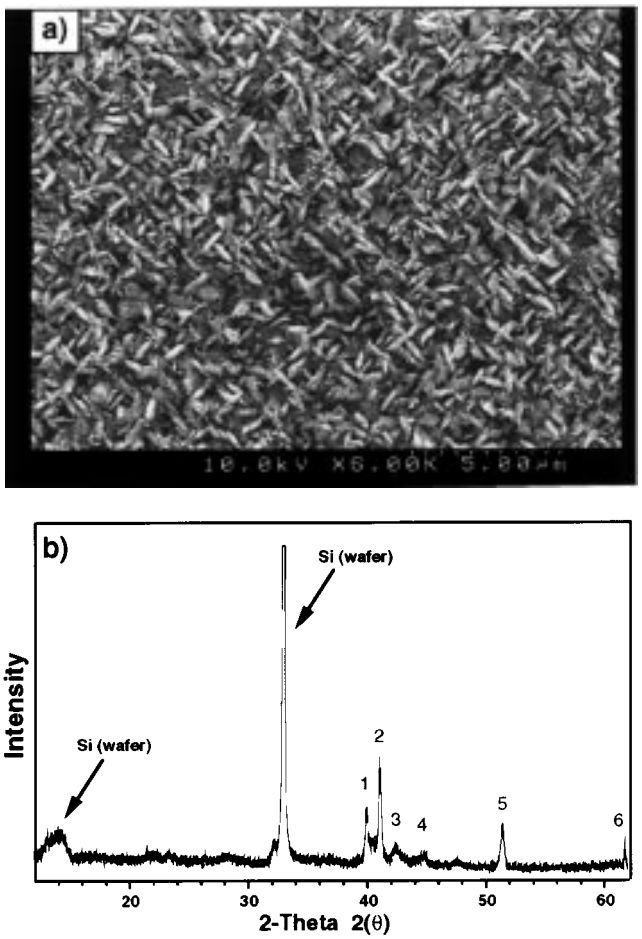

Figure 6. (a) SEM image of sample R22 grown on Si⟨100⟩ at 600 °C showing two preferred growth orientations orthogonal to each other. (b) XRD spectrum of sample showing that titanium silicides (Ti_xSi_y) have formed. At 600 °C, the deposited Ti reacted with the silicon substrate to form titanium silicides, as has been previously reported in the literature.[20] See Table 2 for identification of the numbered peaks.

Sample R22 was run at 600 °C on a Si⟨100⟩ substrate. The resulting film is very different from the previously described runs (Samples R23, R11 and R23W) both in morphology and in chemical composition. A SEM image of the resulting film morphology is shown in Figure 6a, showing two preferred growth orientations which are orthogonal to each other. The "needlelike" shape of the crystallites was a clue that the chemical composition of the film was also different from the previous sample runs. XRD of the film confirmed that no salt was present and that titanium silicides had formed (Figure 6b and Table 2). The higher temperature prevented the deposition of salt, which is consistent with our thermodynamic model. Analysis of the XRD spectrum (see Table 2) revealed that titanium and multiple phases of titanium silicides (TiSi, $TiSi_2$, Ti_5Si_3, Ti_5Si_4) were present. Additional work would be needed to positively identify *all* the crystalline phases of the titanium silicides present in the film, and such a determination is beyond the scope of this paper. The conversion of titanium deposited on silicon substrates to titanium silicides is very important to the microelectronics manufacture, and this process is well-documented in the literature at temperatures exceeding 450 °C.[20] Sodium is an impurity of great concern in microelectronics manufacture,[21] and therefore, our process for depositing titanium silicides would need considerable work before being considered for such applications. A Raman spectrum of sample R22 further confirmed the presence of titanium silicide ($TiSi_2$ in the C49 phase; the other silicide phases were not detected in the Raman spectrum), as well as some Ti_2O_3. Given the surface sensitive nature of Raman spectroscopy, it is not surprising that small amounts of unreacted Ti could convert to titanium oxides, especially given that the Raman technique involved some sample heating from the incident laser in an air environment.

Table 2. XRD Analysis of Sample R22

peak[a] figure 2b	peak position (2θ)	compd	PDF ref no.[b]	PDF ref position (2θ)	crystal orient. (h,k,l)
1	40.0	$TiSi_2$	10-0225	39.3	(060)
		Ti	44-1294	40.2	(010)
		$TiSi_2$	10-0225	40.4	(131)
2	41.1	Ti_5Si_3	29-1362	41.0	(211)
		TiSi	12-0424	41.2	(211)
		Ti_5Si_4	27-0907	41.6	(115)
3	42.4	Ti_5Si_4	23-1079	42.0	(124)
		Ti_5Si_3	29-1362	42.0	(300)
		$TiSi_2$	35-0785	42.2	(040)
		Ti_5Si_4	27-0907	42.2	(214)
		Ti_5Si_3	29-1362	42.7	(112)
		Ti_5Si_4	23-1079	42.7	(006)
4	44.8	Ti_5Si_4	27-0907	44.2	(223)
		Ti_5Si_3	29-1362	45.1	(202)
		TiSi	17-0424	45.3	(301)
		Ti_5Si_4	23-1079	45.3	(025)
5	51.4	Ti_5Si_3	29-1362	51.0	(310)
		Ti_5Si_4	23-1079	51.5	(026)
6	61.7	Ti_5Si_4	27-0907	61.6	(306)
		Ti_5Si_4	27-0907	61.7	(420)

[a] Peak numbers refer to Figure 2b. [b] Powder diffraction file numbers (PDF's) are from the JCPDS International Centre for Diffraction Data.

To confirm that $TiCl_4$ was not directly reacting with the 600 °C silicon surface, Sample R15 was run in the absence of sodium vapor. As expected, EDS and SEM of sample R15 showed that no film formed.

C. Ti Deposited on Cu Substrates. Copper was chosen as the next substrate material since it could be heated to 610 °C and does not readily form titanium alloys at this temperature.[22] The copper substrates were prepared by polishing with 1 μm Al_2O_3 slurry prior to deposition. Sample R26 (see Table 1) was run with a substrate temperature of 610 °C and 1.0×10^{-3} sccm $TiCl_4$ vapor. The 610 °C substrate temperature and the lower concentration of $TiCl_4$ acted to reduce salt deposition relative to samples R11 and R23 (See Figure 5). Visual inspection of the substrate showed that the color changed from copperlike before deposition to steel gray after deposition, which is the color of bulk titanium metal. SEM images of sample R26 are shown in Figure 7a–c. An EDS spectrum taken of this film (see Figure 7d) shows clearly the presence of titanium. Further-

(20) Saenger, K. L.; Cabral, C., Jr.; Clevenger, L. A.; Roy, R. A. *J. Appl. Phys.* 1995, *77*, 5156. Jeon, H.; Sukow, C. A.; Honeycutt, J. W.; Rozgonyi, G. A.; Nemanich, R. J. *J. Appl. Phys.* **1992**, *71*, 4269. Taubenblatt, M. A. Ph.D. Thesis, Stanford University, 1985.

(21) Achutharaman, R.; Hey, P.; Regolini, J. L. *Semiconductor Int.* **1996**, *9*, 149. Maury, D.; Rostoll, M. L.; Gayet, P.; Regolini, J. L. *J. Vac. Sci. Technol. B* **1997**, *15*, 133.

(22) Murray, J. L *Phase Diagrams of Binary Titanium Alloys*; ASM International: Metals Park, OH, 1987. Note that some Ti_xCu_y alloying may occur at the Ti film/Cu substrate interface.

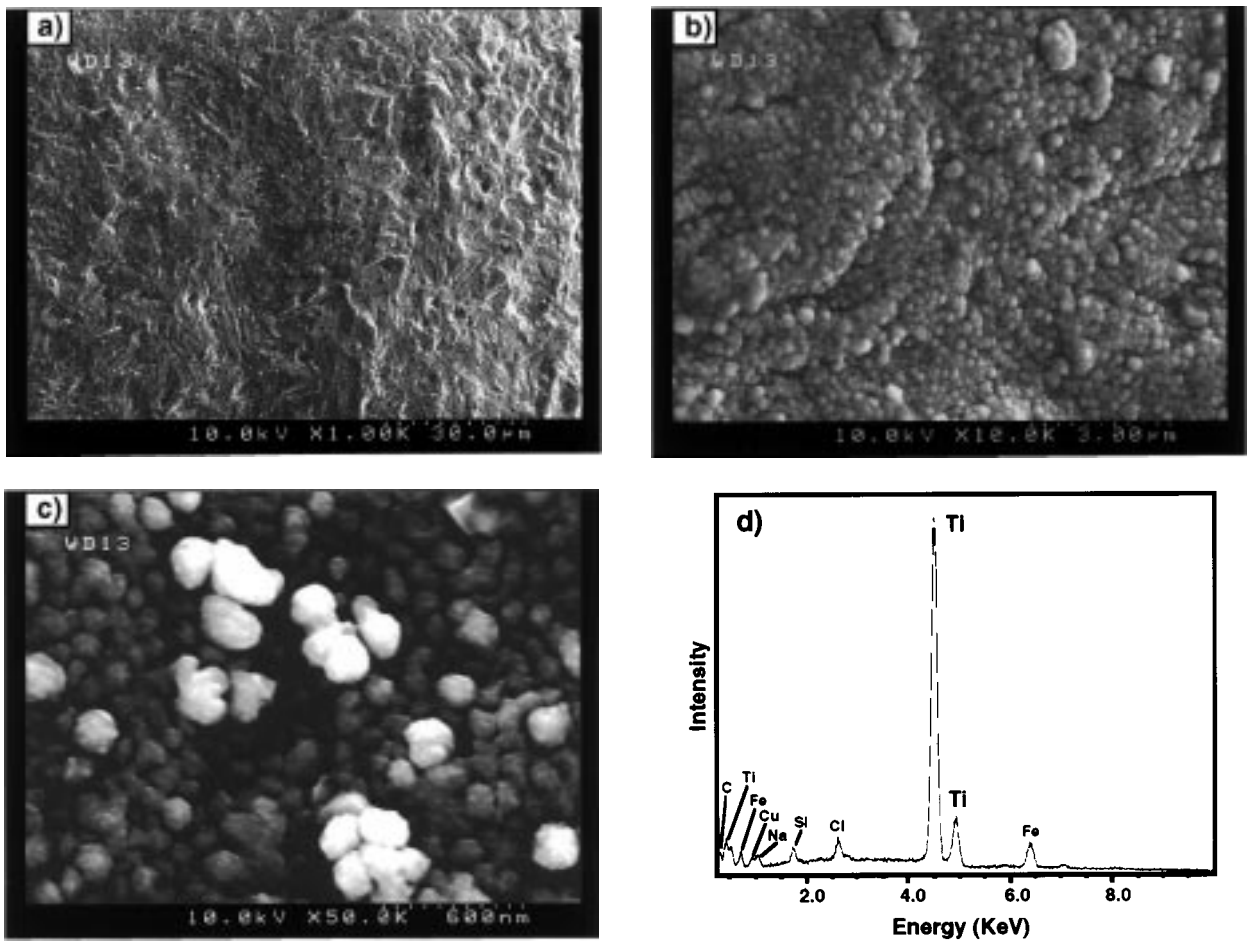

Figure 7. SEM images of sample R26 (grown on OFHC copper substrate at 610 °C) taken at (a) image magnification of 1000; (b) image magnification of 10 000; (c) image magnification of 50 000; (d) EDS spectrum of film shows clearly the presence of titanium, trace signals of Cu, Na, Si, Cl and Fe, and no oxygen signal.[23] The Cu signal is from the substrate and the weakness of the signal is due to the titanium overlayer. An EDS beam energy of 10 keV was used.

more, the EDS showed only trace signals of Cu, Na, Si, Cl, and Fe.[23] The presence of Fe and Si are likely to be the result of impurities in the stock $TiCl_4$ used for all of these experiments (99.9% purity). The XRD spectrum of sample R26 produced only a noisy signal absent of all peaks (including Ti and/or NaCl). One reason for this could be due to the film being polycrystalline with very small grain size. The experimental difficulty in obtaining an XRD titanium signal from sample R26 was in part due to the inherently more noisy copper substrate (as compared with the single-crystal silicon substrates for which obtaining a Ti signal was possible).

To further characterize sample R26, images were taken with a field emission gun TEM with both EDS and SAED capabilities. The TEM grid (C film on Cu grid) was prepared by passing it through an alcohol suspension containing film scrapings which were removed from the film with a carbide scribe. The TEM showed that film consisted of densely packed 100−300 nm crystallites. SAED showed that the sample was polycrystalline, while EDS showed that the primary signal was from Ti.

(23) Signal intensity of individual elements in the EDS spectrum does not directly correlate to the percent amount present in the sample, and low energy peaks are often discriminated against (they are of lower intensity) versus peaks located at about half the incident electron beam energy.

D. TiN Deposited on Cu. To further illustrate the versatility of the coflow sodium metal/metal halide CVD reactor, an experiment was performed which demonstrated that a ceramic titanium nitride film could also be produced. Titanium nitride was chosen due to the simplicity of the reaction chemistry (see eq 3) and because it is of interest to the machine-tooling industry for extending the useful lifetime of machine-cutting tools.[3] By simply adding 85 sccm of nitrogen gas to the argon flows (see reactions 2 and 3), a titanium nitride film was produced. It should be noted that when the Ar dilution gas was used in its unpurified state (containing 3−6 H_2O/O_2 molecules per 1×10^6 argon atoms) TiO_2 films were readily formed on both copper and silicon substrates for reaction 2.

The aim of the experiment was to grow a salt-free TiN film using a polished oxygen-free high-conductivity (OFHC) copper substrate material. Sample R29 was run with a substrate temperature of 610 °C and 3.3×10^{-3} sccm of $TiCl_4$ vapor and 5.3×10^{-2} sccm of Na vapor (see Table 1). Shown in Figure 8a,b are the SEM images of the resulting film. Figure 8b shows clearly that the film consists of cubic crystallites with an edge length of ~60 nm. The crystallites also appear to form stacks, an indication that surface growth is indeed occurring. A TEM grid was prepared in a manner similar to that previously described for R26. A selected

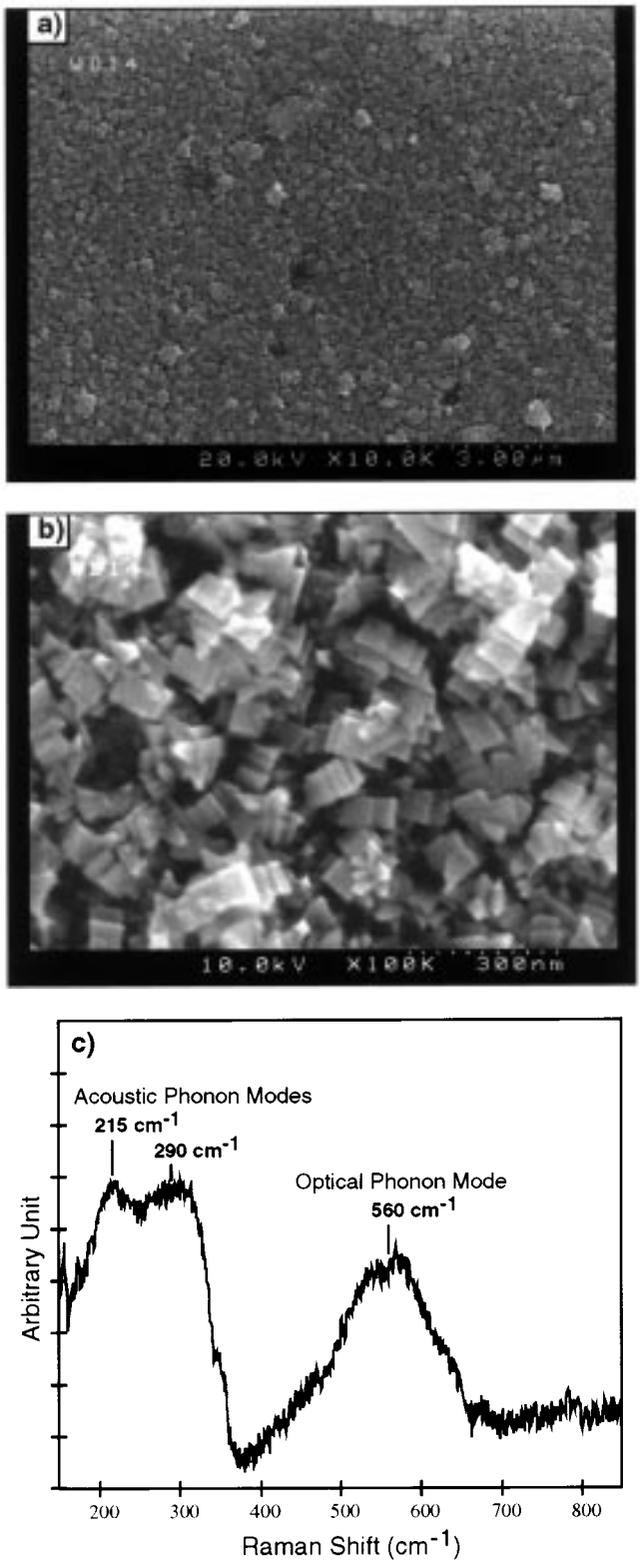

Figure 8. SEM images of sample R29 deposited on a OFHC copper substrate at 610 °C showing (a) image magnification of 10 000 and (b) image magnification of 100 000. Figure 8b shows clearly that the film consists of cubic crystallites with an edge length of ~60 nm. (c) Raman spectrum of sample R29 showing that the deposited material is titanium nitride. The peaks at 215 and 290 cm^{-1} correspond to the acoustic phonon modes of TiN previously measured to be 200 and 280 cm^{-1} respectively.[24] The peak at 560 cm^{-1} corresponds to the optical phonon mode of TiN previously measured to be 520−550 cm^{-1}.[24]

Table 3. Potential Films Which Can Be Grown with the Sodium/Metal Halide CVD Reactor vs Conventional Thermal CVD

proposed film material	temperature, °C: conventional CVD	temperature, °C: this method	reactant feedstock for the metal halide in eq 1
Ti	950−1100	610	$TiCl_4$
TiC	950−1100	610	$TiCl_4$ and CCl_4
Si	950−1080	610	$SiCl_4$ or $SiHCl_3$
Ta	900−1000	610	$TaCl_5$
TiB_2	950−1100	610	$TiCl_4 + BCl_3$
SiC	>1100	610	$SiCl_4 + CCl_4$ or $SiHCl_3 + CCl_4$

area diffraction pattern showed that a polycrystalline film had been produced, while EDS revealed the presence of Ti, Cu, Fe, O, N, and C. Copper and carbon signals are from the TEM grid (or from the Cu substrate) and Fe, C, and O only appeared in trace signal levels. There was no evidence of Na or Cl (within the 1.0−0.2 wt % detection limit for EDS), which confirmed that an essentially salt-free titanium nitride film has been successfully deposited.

A Raman spectrum of the TiN sample is shown in Figure 8c. This figure shows peaks at 215, 290, and 560 cm^{-1}. The peaks at 215 and 290 cm^{-1} correspond to the acoustic phonon modes of TiN, which are in excellent agreement with the previously measured values of 200 and 285 cm^{-1} for TiN_x, where $x = 0.995$.[24] The peak at 560 cm^{-1} corresponds to the optical phonon mode of TiN previously measured to be from 520 to 550 cm^{-1} for TiN_x, where $x = 0.995$.[24] Furthermore, the presence of Ti_2O_3, TiO_2, and TiO were not detected in the Raman spectrum. If TiO_2 was present (in even small amounts), it would have been readily detected due to fact that it is noncubic and highly polarizable (it is a strong Raman scatterer) in comparison with stoichiometric cubic TiN (for which first-order scattering is forbidden).[25]

Summary and Conclusions

We have successfully demonstrated that metal and ceramic thin films can be produced at low temperatures through the reaction of alkali metal vapor with metal halide vapor in a low-pressure coflow diffusion reactor. Using this technique, we have successfully produced essentially salt-free titanium and titanium nitride films on copper substrates heated to 610 °C, which is a very favorable temperature compared to conventional CVD process for depositing titanium of 900−1200 °C.[5] Attempts to grow titanium films on Si⟨100⟩ substrates at 600 °C produced titanium silicide films. At lower temperatures (260 °C), composite salt/Ti films were grown on the silicon wafers.

The low-pressure coflow sodium metal vapor/metal halide reactor CVD process promises to be a new method for thin film growth and has the attraction of being of lower operational temperature than many conventional CVD routes. Furthermore, this technique should be general for the deposition of a wide class of ceramic and metallic thin films. For example, by switching the metal halide, a wide variety of thin film materials could be

(24) Spengler, W.; Kaiser, R.; Christensen, A. N.; Muller-Vogt, G. *Phys. Rev. B.* **1978**, *17*, 1095.
(25) Zhang, H.; Kisi, E. H.; Myhra, S. *J. Phys. D. Appl. Phys.* **1996**, *29*, 1367.

easily grown (see Table 3). Finally, this new technique for thin film growth has the additional benefit that the salt byproduct is easily removed from the process stream and is environmentally benign.

Acknowledgment. The authors wish to give special thanks to Dr. Ryna Marinenko, Dr. Sheryl Ehrman, Mr. James Allen, and Dr. Eric Steel, for their assistance with WDS, TEM, SEM, and XRD sample analysis interpretation, and Mr. Raymond Fink and Mr. Douglas. P. DuFaux, for their assistance in the building and design of the low-pressure coflow reactor. This research was conducted while J.H.H. held a NIST NRC postdoctoral fellowship.

CM980161Q